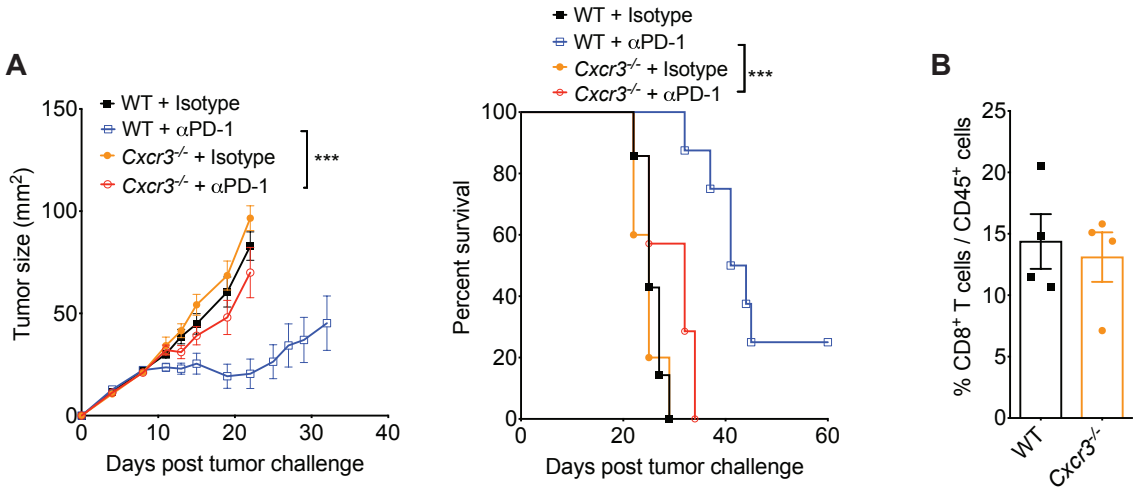

Figure S1. Related to Figure 1. CXCR3 is necessary for the response to PD-1 blockade therapy in the D4M.3A.3 UV3 melanoma model. (A) WT and *Cxcr3*$^{-/-}$ mice were inoculated subcutaneously with 5x10^5 D4M.3A.3 UV3 tumor cells, and on days 8, 11 and 14 after tumor inoculation, mice were intraperitoneally treated with 200µg of either isotype control or anti-PD-1 antibodies. Tumor growth and survival were monitored until the experimental end-points. Tumor growth in WT and *Cxcr3*$^{-/-}$ mice treated with isotype or anti-PD-1 antibodies (n=5-8 mice per group). Data are presented as the mean ± SEM; ***p<0.001, with statistical significance determined by two-way ANOVA. Survival curves of the percentage of mice whose tumor sizes were <100mm^2 at each time point. Statistical differences in survival were assessed by a Mantel-Cox log-rank test (***p<0.001). Representative data are shown from two independent experiments. (B) Quantification of CD8$^+$ T cell frequencies within tumors of WT and *Cxcr3*$^{-/-}$ mice on day 8 after D4M.3A.3 UV3 tumor inoculation. Representative data are shown from two independent experiments.

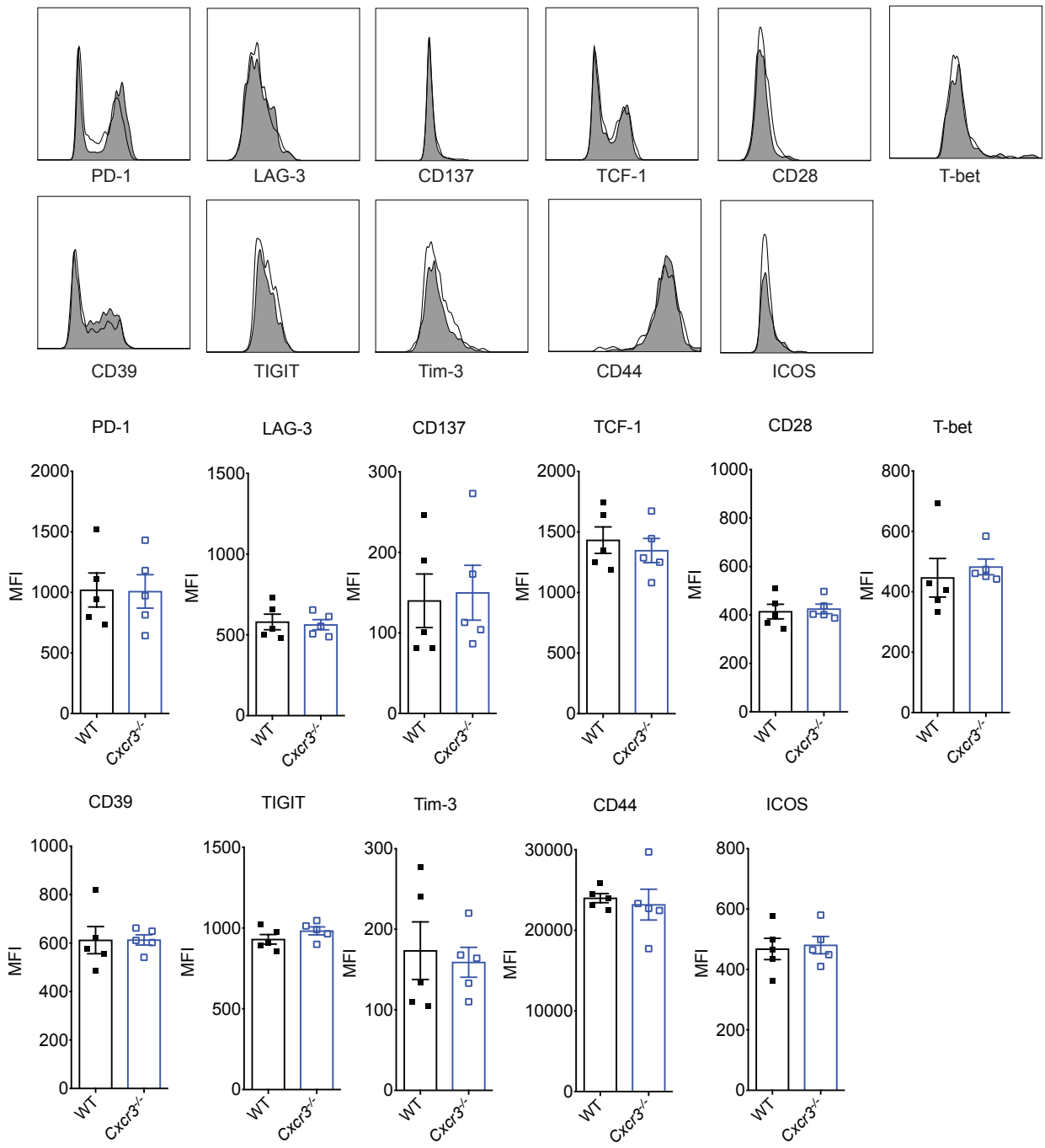

Figure S2. Related to Figure 1. Intratumoral CD8⁺ T cells from untreated WT and *Cxcr3*$^{-/-}$ mice show comparable levels of activation and dysfunction. Representative histograms showing the expression of various surface markers and transcription factors on CD8⁺ T cells within tumors of WT (line histograms) and *Cxcr3*$^{-/-}$ mice (filled histograms) on day 8 after MC38 tumor inoculation. Bar graphs represent the mean values of the indicated data points, and the error bars represent SEM. The data shown are representative of two independent experiments.

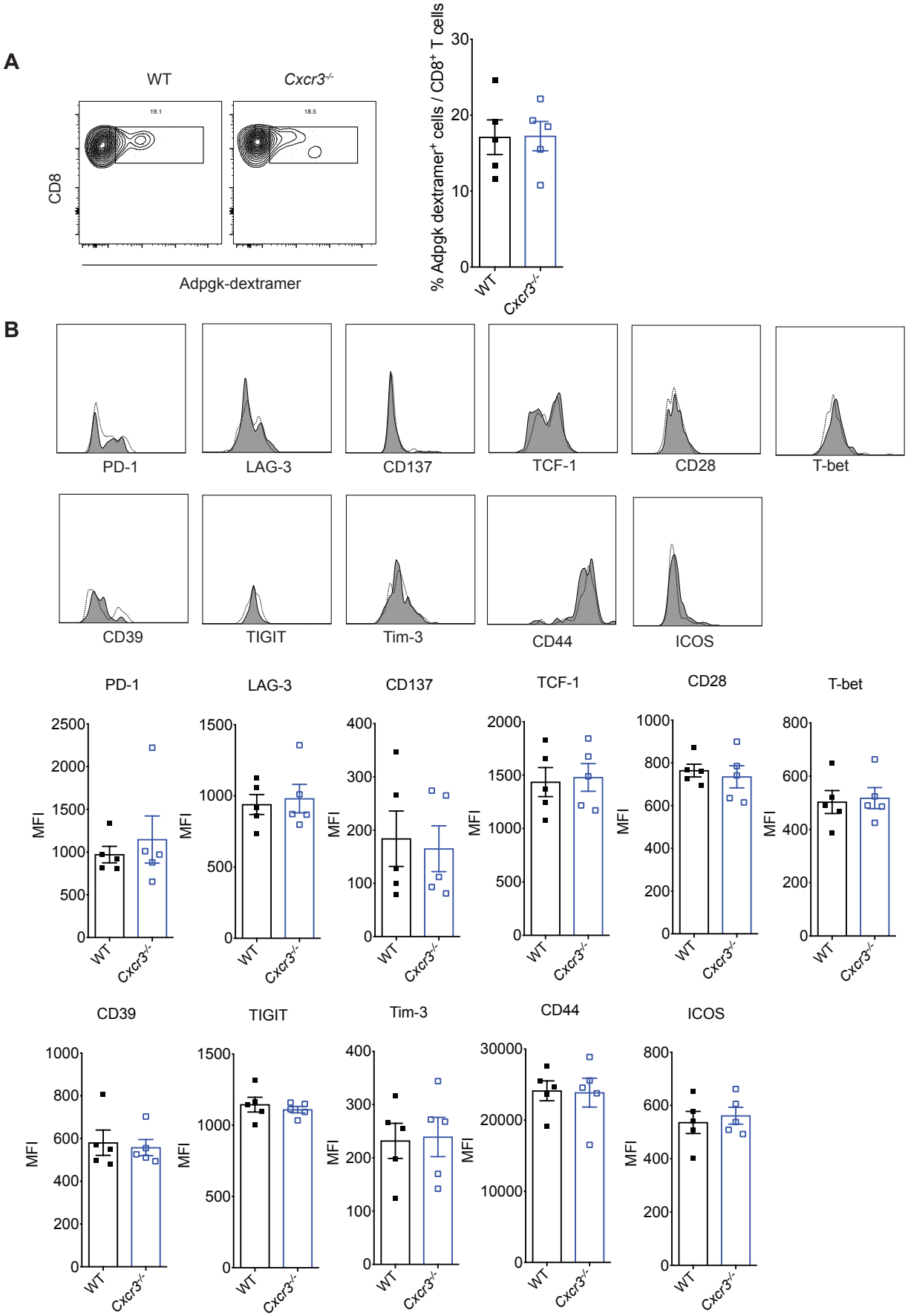

Figure S3. Related to Figure 1. Intratumoral tumor antigen-specific CD8⁺ T cells from untreated WT and *Cxcr3*$^{-/-}$ mice show comparable levels of activation and dysfunction. (A) Quantification of tumor antigen-specific CD8⁺ T cell frequencies within tumors of WT and *Cxcr3*$^{-/-}$ mice on day 8 after MC38 tumor inoculation. (B) Representative histograms showing the expression of various surface markers and transcription factors on tumor antigen-specific CD8⁺ T cells within tumors of WT (line histograms) and *Cxcr3*$^{-/-}$ mice (filled histograms) on day 8 after MC38 tumor inoculation. Bar graphs represent the mean values of the indicated data points, and the error bars represent SEM. The data shown are representative of two independent experiments.

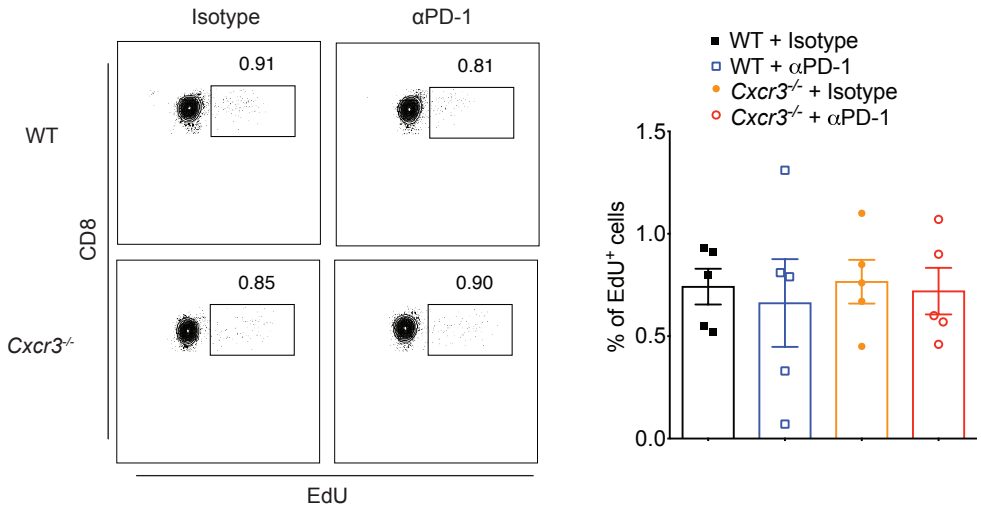

Figure S4. Related to Figure 2. Proliferative response of CD8⁺ T cells in the draining lymph node after anti-PD-1 treatment. Groups of WT and *Cxcr3*$^{-/-}$ were inoculated subcutaneously with 1×10^{6} MC38 on day 0. Following tumor inoculation, tumor-bearing mice were intraperitoneally treated with FTY720 (1mg/kg) on days 7 and 9 as well as either isotype or anti-PD-1 antibodies (200μg) on day 8. Administration of EdU (50mg/kg) was performed on day 10, followed by quantification of EdU⁺ CD8⁺ T cells within draining lymph nodes on day 11. Contour plots and bar graphs reflect the proportion of EdU⁺ cells out of total CD8⁺ T cells in draining lymph nodes. Bar graph represents the mean value of the indicated data points; error bars represent SEM. Representative data are shown from two independent experiments.

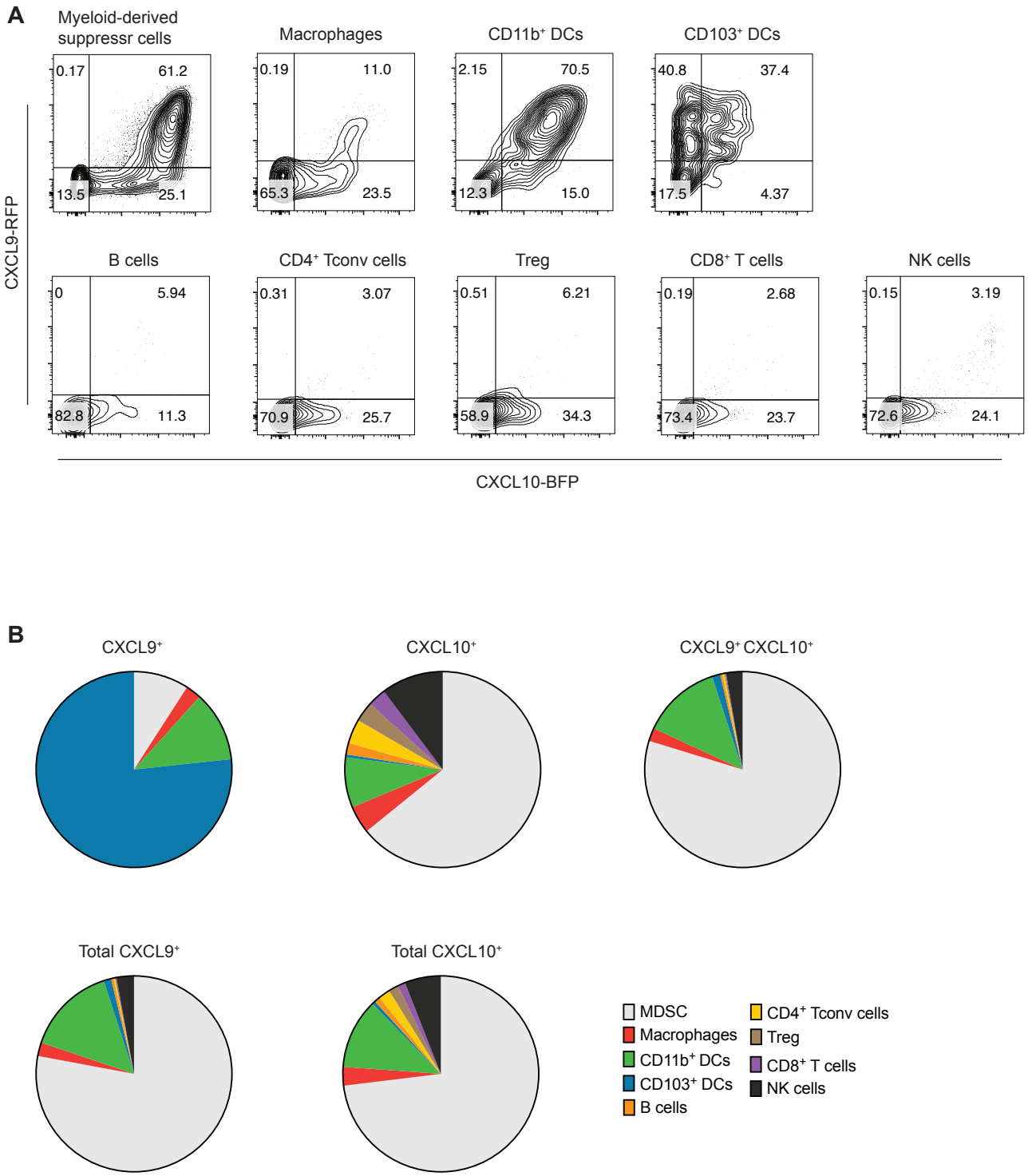

Figure S5. Related to Figure 5. Identification of CXCR3 ligand-producing cells within tumors. (A) Expression of CXCL9 and CXCL10 on myeloid-derived suppressor cells (MDSC) (CD11b$^+$ Gr-1$^+$), macrophages (Gr-1$^-$ CD11c$^-$ CD11b$^+$ F4/80$^+$), CD11b$^+$ DC (Gr-1$^-$ CD11c$^+$ MHCII$^+$ CD11b$^+$), CD103$^+$ DC (Gr-1$^-$ CD11c$^+$ MHCII$^+$ CD103$^+$), B cells (CD19$^+$), CD4$^+$ conventional T cells (Tconv) (CD3$^+$ CD4$^+$ CD25$^-$), regulatory T cells (Treg) (CD3$^+$ CD4$^+$ CD25$^+$), CD8$^+$ T cells (CD3$^+$ CD8$^+$) and NK cells (CD3$^-$ NK1.1$^+$) in MC38 tumors on day 8 was analyzed by flow cytometry *ex vivo*. (B) The percentages of various immune cell subsets were compared in the CXCL9 single-producing, CXCL10 single-producing, CXCL9-CXCL10 double-producing, total CXCL9-producing and total CXCL10-producing cell populations.

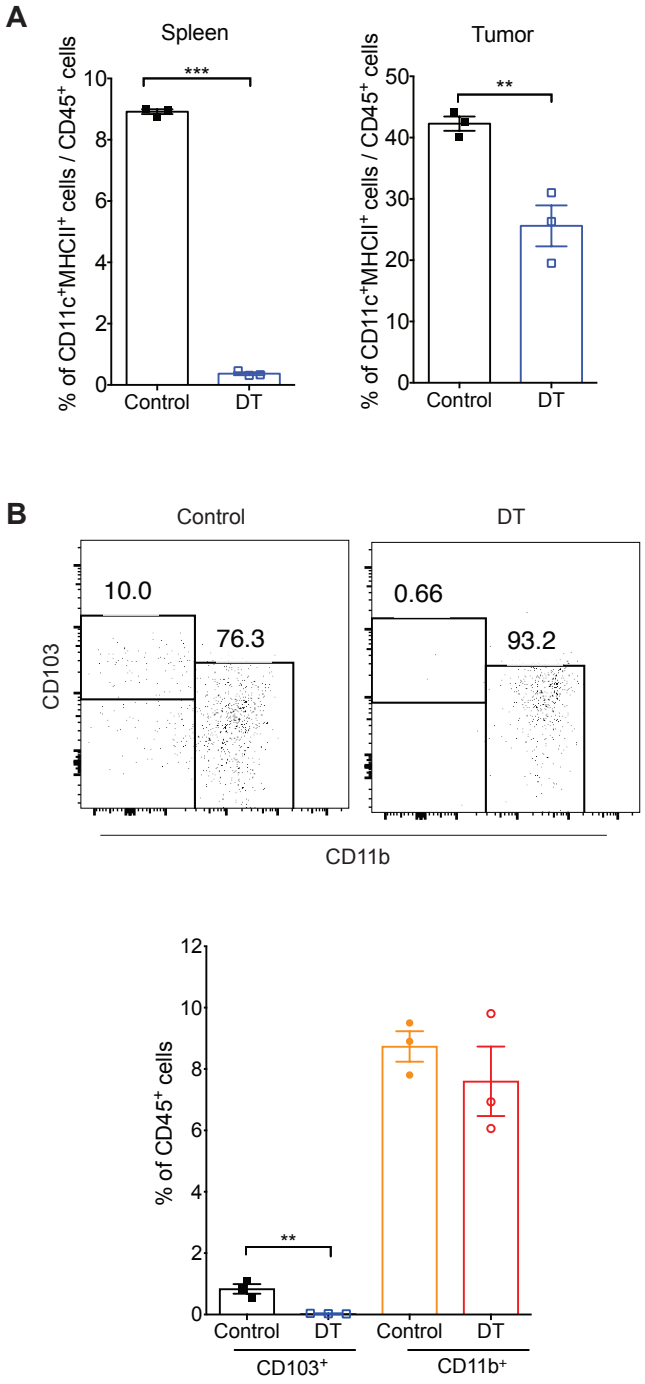

Figure S6. Related to Figure 5. Diphtheria toxin treatment in WT mice reconstituted with *Zbtb46*^{DTR} bone marrow preferentially depletes CD103$^+$ DC within tumors. (A) Percentage of CD11c$^+$ MHCII$^+$ DCs out of total CD45$^+$ cells within the spleens and tumors of WT mice reconstituted with *Zbtb46*^{DTR} bone marrow and treated with either a vehicle control or diphtheria toxin (DT). Bar graphs represent the mean values of the indicated data points, and the error bars represent the SEM; ***p*<0.01; ****p*<0.001, with statistical significance determined by Student's *t*-test. (B) Representative FACS plots of CD103$^+$ DC and CD11b$^+$ DC subsets within tumors of WT mice reconstituted with *Zbtb46*^{DTR} bone marrow and treated with either vehicle control or DT. Bar graph showing the percentage of CD103$^+$ DCs and CD11b$^+$ DCs out of total CD45$^+$ cells within tumors of WT mice reconstituted with *Zbtb46*^{DTR} bone marrow and treated with either a vehicle control or DT. Data are mean ± SEM; ****p*<0.001, with statistical significance determined by Student's *t*-test. Data are representative of two independent experiments.

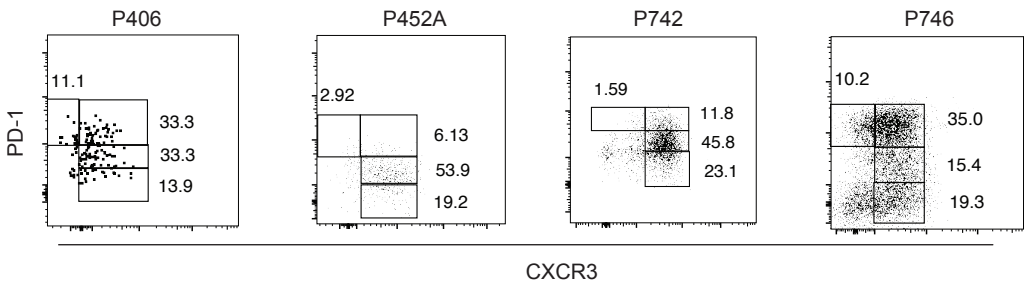

Figure S7. Related to Figure 7. Identification of four subsets of dysfunctional CD8$^+$ T cells in human melanomas. Flow plots reflect the proportion of different subsets of CD8$^+$ T cells within tumors based on the cell surface expression of CXCR3 and PD-1 in melanoma patients.

Table S1. Related to Figure 7. Patient characteristics. Patient characteristics including age at time of treatment start, sex, type of treatment received (Pembro, Pembrolizumab; NIVO, Nivolumab; IPI, Ipilimumab) and response to treatment. All patients classified as responders (R) showed clear radiographic decrease in disease and maintained an ongoing response without progression through to last follow-up. Patients classified as non-responders (NR) did not respond to treatment radiographically and had clear and rapid progression. Progression free survival (pfs) is given in days from treatment start to radiographic scan when progression was first noted. Blood was collected prior to initiation of therapy (between 9 days prior to therapy and the day of therapy initiation) and post-treatment blood collection occurred between 19 and 93 days (median = 42) after initiation of therapy.

patient	age	sex	treatment	response	pfs	plasma_Pre	plasma_Post
327	57	M	Pembro	R	ongoing response	0	42
471	59	M	Pembro	R	ongoing response	0	NA
509	47	M	Pembro	R	ongoing response	0	42
525	79	M	Pembro	R	ongoing response	0	42
545	78	M	Pembro	R	ongoing response	-9	22
546	79	M	Pembro	R	ongoing response	0	NA
547	75	M	Pembro	R	ongoing response	-1	41
567	59	M	Pembro	R	ongoing response	0	40
628	68	F	Pembro	R	ongoing response	0	42
642	64	M	Pembro	R	ongoing response	0	42
654	70	F	IPI+NIVO	R	ongoing response	-6	44
694	73	M	IPI+NIVO	R	ongoing response	0	42
697	59	M	IPI+NIVO	R	ongoing response	0	42
698	60	M	Pembro	R	ongoing response	0	43
699	39	F	Pembro	R	ongoing response	0	44
707	87	F	Pembro	R	ongoing response	0	19
730	70	M	pembro	R	ongoing response	0	42
733	51	M	IPI+NIVO	R	ongoing response	0	42
584	67	F	IPI+NIVO	NR	230	0	41
594	63	F	IPI+NIVO	NR	78	0	42
596	46	F	IPI+NIVO	NR	126	0	35
603	28	M	IPI+NIVO	NR	291	0	46
606	63	F	Pembro	NR	43	0	44
649	58	F	IPI+NIVO	NR	83	0	42
662	57	F	Pembro	NR	52	0	93
709	72	F	Pembro	NR	49	0	49
728	70	F	NIVO (adjuvant)	NR	78	0	42
737	74	F	IPI+NIVO	NR	100	-1	37